IEEE Access
Multidisciplinary | Rapid Review | Open Access Journal

Received 19 March 2024, accepted 15 May 2024, date of publication 24 May 2024, date of current version 4 June 2024.

Digital Object Identifier 10.1109/ACCESS.2024.3405182

RESEARCH ARTICLE

Real-Time Management of Coal Mine Underground Shield Machine Digging Speed Based on Improved Residual Neural Networks

HUIGANG XU[1,2], XUYAO QI[1,2], AND ZHONGQIU LIANG[3]
[1]School of Safety Engineering, China University of Mining and Technology, Xuzhou 221116, China
[2]Key Laboratory of Gas and Fire Control for Coal Mines, China University of Mining and Technology, Xuzhou 221116, China
[3]CCTEG Shenyang Research Institute, Shenyang 113122, China

Corresponding author: Huigang Xu (XHG20240115@163.com)

ABSTRACT Aiming at the lack of accuracy and effectiveness of the current shield machine speed prediction method, the study proposes to improve the residual network and combine this improved algorithm with the surrounding rock category prediction model to construct the underground shield machine digging speed prediction model. With an average accuracy of 87.4%, an F1 value of 0.86, and an accuracy of 0.84, the study's prediction model of surrounding rock categories was determined to be valid and superior to the other compared models. The effectiveness of the improved residual algorithm constructed by the study was verified, and it was found to have a better fit to the actual values, with a maximum deviation error value of 4.6 mm/min and a root mean square error of 1.835, which was lower than the other comparative algorithms. The empirical analysis of the underground shield machine digging speed prediction model constructed by the study revealed that the area under the line of the work characteristic curve of the subjects was 0.74, and the F1 value was 0.35, and the accuracy was as high as 84.6%, which was significantly better than that of other comparative models. The shield machine digging speed prediction model, which is based on an enhanced residual network built in the study, performs better than other comparison models, according to the results, which can serve as a theoretical guide for the digital management of coal mine output.

INDEX TERMS Residual neural network, shield machine, digging speed, real-time management, surrounding rock type.

I. INTRODUCTION

As one of the important equipment of modern mine mining technology, the underground shield machine (SM) is increasingly widely used in underground projects. The digging speed (DS) of SM is directly related to the progress and efficiency of the whole project, so how to manage the DS of SM in real time has become a key issue to improve the efficiency and safety of mine mining [1]. However, the old approach of DS management of SM finds it challenging to satisfy the actual need as coal mining depth and mine complexity develop. The traditional methods are mainly based on experience and rules, which have problems such as low accuracy and difficult to adapt to the complex environment [2]. Residual neural network (ResNet), as a deep neural network architecture, introduces the concept of residual learning, which improves the training efficiency, learning ability, and generalization ability of DS prediction of SM, and helps to improve the accuracy and stability of prediction [3]. However, traditional ResNet may encounter problems such as gradient vanishing or gradient explosion when training deep networks [4], [5]. A recurrent neural network (RNN) variation called long short-term memory (LSTM) is appropriate for processing time-series data and is good at capturing long-term dependencies in data [6]. In shield DS prediction, the improvement of ResNet by combining LSTM can better deal with long-term dependencies in time series data, which is conducive to better capturing the temporal characteristics of the data and more

The associate editor coordinating the review of this manuscript and approving it for publication was Shadi Alawneh.

comprehensively capturing the complex patterns in shield DS prediction [7]. However, there are fewer studies that utilize LSTM to improve ResNet and apply it to shield DS prediction. Thus, the study suggests combining LSTM with ResNet to create a shield DS prediction model based on enhanced ResNet in order to close this gap, achieve the intelligent and accurate management of DS of SM, and increase the efficiency of coal mining. The innovation of the research is the development of a new shield DS prediction method. The contribution of the research is to provide an advanced technical means for coal mine production management by improving coal mine production efficiency, ensuring work safety and reducing costs. The study describes the current status of DS management in ResNet and SM in section one, and constructs the geotechnical grade prediction model (GGPM), improved ResNet algorithm and DS prediction model based on improved residual network algorithm for underground SM in coal mines in section two. The proposed GGPM model, improved ResNet algorithm and the DS prediction model based on improved residual network algorithm are empirically analyzed in section three. Conclusion and outlook of future research directions are presented in Section IV.

II. RELATED WORKS

As computer science advances, ResNet has created a multitude of uses in an increasing number of domains. Xue et al. introduced a unique self-supervised learning technique based on ResNet, to enable automatic learning of video representations. Their suggested self-supervised learning approach was found to be effective and to have some degree of generalizability when utilized as an efficient pre-training technique for the job of identifying the activities in the video [8]. Salama et al. suggested a ResNet-based breast cancer medical image-assisted diagnosis model and confirmed the model's efficacy. The model's diagnostic accuracy, sensitivity, and precision were determined to be 97.51%, 96.51%, and 96.78%, respectively [9]. To improve the performance of fruit harvesting robots, Lawal et al. proposed a ResNet-based fruit detection model to improve the detection accuracy of fruits and other crops, and validated the effectiveness of the model. It was discovered that, in comparison to the conventional model, its average detection accuracy was 89.3% and its detection speed was 96.8 frames per second. These results could be used to enhance fruit harvesting robots [10]. Chen et al. suggested a ResNet-based classification and identification model for near-infrared spectroscopy in order to establish a method for efficiently determining the species and duration of storage for sliced lentils utilizing this technique for the safe storage and management of porcini mushrooms. The model's validity was confirmed, and its accuracy for species classification and storage duration was greatly enhanced. This makes the model practically applicable to the porcini mushroom supply chain [11]. Yang used real-time pulse sequence low-quality pure displacement NMR data for efficient collection, and ResNet was used to analyze and process the data. The validity of the method was verified and it was found that the method can perfectly eliminate noise and artifacts and smooth the baseline, and it can greatly facilitate various NMR applications [12].

The field of DS management in SM is seeing an increasing number of methods used to it due to the rapid development of information technology. To facilitate tunnel excavation in SM, Fang et al. proposed 2D and 3D finite element evaluations of the system based on initial soil anisotropy and non-coaxial plasticity. It was discovered that the degree of cross anisotropy and the excavation technique work together to provide an accurate estimate of the tunnel's maximum vertical displacement, hence these two variables must be taken into account when excavating SM tunnels [13]. Gao et al. suggested a digitization-based technique to quickly acquire the delayed uni-axial compressive strength for subterranean projects with complex geological conditions so that the excavation speed and support design may be adjusted. The validity of the method was verified, and it was found that the drilling parameters had a high responsiveness to the rock unconfined compressive strength, which could be used to conduct continuous and rapid testing of the surrounding rock unconfined tensile strength [14]. Zhang et al. proposed an analytical model based on elliptically convergent deformation patterns in order to accurately predict shield excavation effects. The validity of the model was verified and it was found to be an alternative method for conservatively estimating the effects of tunnel excavation in saturated soils for preliminary design [15]. Jasemi et al. suggested a speed prediction system based on a multilevel cell spin transfer moment random access memory. The validity of this system was verified, and it was found that the system may keep the error rate below 0.12%, which is valuable for practical application [16]. Wang et al. suggested a shield construction advancement model based on LSTM RNNs in an effort to increase the shield building advancement rate. After the model's validity was confirmed, it was discovered that the measured and projected values had a strong correlation (a correlation coefficient of 0.93), which has practical applications in the development of shields [17].

The aforementioned study amply illustrates how ResNet has been implemented in numerous domains and how different approaches are utilized in the SM tunneling space. Nevertheless, there is still need for development in terms of accuracy and precision, and the current DS prediction model of SM is unable to satisfy the demands of real-time monitoring. Therefore, in order to deal with the DS data of SM more effectively and realize real-time management and monitoring, the study proposes to construct an improved residual network based on LSTM and apply the improved algorithm in the field of DS prediction of SM.

III. DIGGING SPEED PREDICTION MODEL OF UNDERGROUND COAL MINE SHIELD MACHINE BASED ON IMPROVED RESNET

To enhance the feasibility and effectiveness of DS prediction of SM, the study proposes to improve the ResNet

algorithm based on LSTM, utilizes the GGPM model of coal mine underground using XGBoost, and combines the GGPM model with the improved ResNet structure to build the DS prediction model of coal mine underground SM.

A. XGBOOST-BASED GGPM MODEL FOR UNDERGROUND COAL MINES

XGBoost-based coal mine underground GGPM Before shield construction, the study needs to classify the rock and soil of the operation in order to adjust the tunneling parameters according to the level of the tunnel surrounding rock class. To provide direction and references for engineering construction, a variety of methods are currently available for classifying the shield perimeter rock grades [18], [19]. The neural network chosen for the study is the eXtreme gradient boosting (XGBoost) algorithm. XGBoost algorithm is an improved decision tree (DT) algorithm, which can deal with a variety of complex and irregular data [20], [21], [22]. The surrounding rock type (SRT) prediction model constructed by the study is shown in Figure 1.

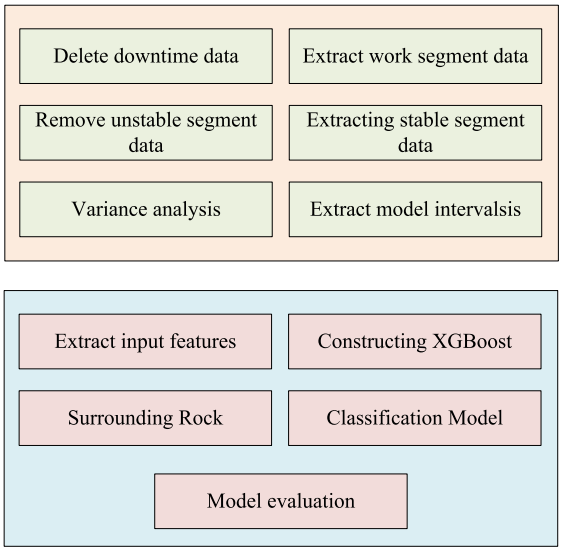

FIGURE 1. Prediction model of surrounding rock category.

As shown in Figure 1, the XGBoost SRT prediction model constructed by the study consists of four parts: data preparation and processing, feature extraction, XGBoost algorithm classification and model evaluation. In the data preparation and processing stage, the study eliminates the data in the downtime segment and screens the data in the stable segment for extraction. Subsequently, the study performed ANOVA on the extracted data to obtain the model intervals. The acquired model intervals are input into the XGBoost algorithm as features, and the study firstly utilized the XGBoost algorithm to sum up the prediction results of multiple DTs, which is calculated as shown in equation (1).

$$\hat{y} = \sum_{k=1}^{K} f_k(x_i), f_k \in F \tag{1}$$

In equation (1), K denotes the DTs, F is the space of DTs. f_k denotes the specific DT and $\hat{y}$ is the output of the algorithm. The features and length of the samples are set, and the expression formula of its input samples is shown in equation (2).

$$D = \{(x_i, y_i)\} \left(|D| = n, x_i \in R^m, y_i \in R\right) \tag{2}$$

In equation (2), K is the DTs. m denotes the features. The formula for calculating the space of DTs, i.e., the possibility of DTs, is shown in equation (3).

$$F = \left\{f(x) = w_q(x)\right\} (q : R^m \to T, w \in R) \tag{3}$$

In equation (3), q denotes the structure of the DT and T denotes the child nodes of the DT. $f(x)$ denotes the DT structure and w denotes the node weights of the DT. Equation (4) illustrates the calculation of the XGBoost algorithm's objective function (OF).

$$\Gamma(\phi) = \sum l(\hat{y}_i, y_i) + \sum_k \Omega(f_k) \tag{4}$$

In equation (4), $\hat{y}_i$ is the sample predicted value and y_i is the actual value. $\Gamma(\phi)$ denotes the loss error. The OF is regularized to prevent the function from over-fitting. The formula is shown in equation (5).

$$\Omega(f) = \gamma T + \frac{1}{2}\lambda \|w\|^2 \tag{5}$$

In equation (5), γ and λ denote the weighting coefficients. Since XGBoost improves the training accuracy of the model by iteratively increasing the weak learners, in order to correct the cumulative difference problem that occurs in the weighting process, the study proposes to utilize the constant term to correct it. At this stage, the XGBoost algorithm's OF is determined, as indicated by equation (6).

$$\Gamma(\phi) = \sum l\left(f_t(x_i) + \left(\hat{y}_i^{(t-1)}, y_i\right)\right) + \sum_k \Omega(f_t) + C \tag{6}$$

In equation (6), C denotes a constant. If the OF is formulated using the leaf nodes (LNs) T and the fraction of LNs w, the OF is formulated as shown in equation (7).

$$\Gamma(t)(\phi) = \left[G_j w_j + \frac{1}{2}(H_j + \lambda) w_j^2\right] + \gamma T \tag{7}$$

In equation (7), G_j denotes the accumulation of the LNs and w_j denotes the accumulation of the LN scores. Subsequently, the study applies the perimeter rock classification model based on XGBoost algorithm in practice, and its application flow is shown in Figure 2.

The study first uses the Python programming language to create the XGBoost model's training and testing environment, as shown in Figure 2. To ensure consistency in the results of each segmentation, the dataset is divided into training and testing sets in a 1:1 ratio. Random seeds are fixed. During the training process, the study uses the sampled and processed balanced training dataset to validate and evaluate the reliability and generalization of the XGBoost model. To maximize

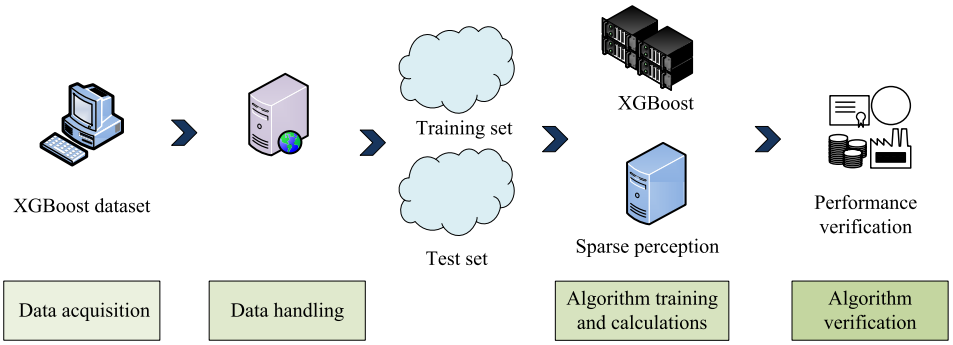

FIGURE 2. Application flow of the XGBoost algorithm.

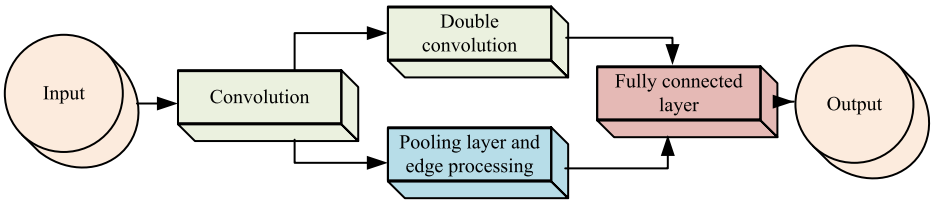

FIGURE 3. The residual neural network's fundamental architecture.

the model's precision rate, the study additionally verifies the model's performance using assessment measures like accuracy, precision, and recall.

B. MODIFIED RESNET ALGORITHM INCORPORATING LSTMS

After completing the construction of the GGPM model for underground coal mines, the study can classify the working geotechnics and select the appropriate SM Hori parameters. Based on the selected SM parameters, the study implements the accurate prediction and intelligent management of the SM speed. The study utilizes ResNet as the basic algorithm for SM speed management. ResNet is a deep learning model proposed by Microsoft Research [23], [24]. The ResNet approach seeks to improve the network's performance and training efficiency by including a residual module that allows the network to learn a residual mapping, or the residual between the input and the desired output [25], [26], [27]. Figure 3 illustrates the fundamental composition of ResNet.

The input layer can receive input data from the outside world and convert it into a form suitable for neural network processing. The convolutional layer, on the other hand, can perform convolutional operations on the input data to extract features, and it is capable of capturing local features in the input data. Equation (8) displays the convolutional network formula.

$$f(x) = act\left(\sum_{i,j}^{n} \theta_{(n-i)(n-j)} x'_{ij} + b\right) \tag{8}$$

In equation (8), act denotes the activation function and θ denotes the weight data. b denotes the bias and x' denotes the sequence data. The purpose of the pooling layer, which typically comes after the convolutional layer, is to condense the feature map while maintaining the salient characteristics. To expedite the process of training and inference for the model, the pooling procedure serves to lessen the sensitivity of the model to location while also minimizing its computational effort. Equation (9), which illustrates how ResNet uses the output of the previous layer as the input to the next layer for feature extraction and fusion, is the pooling layer.

$$x_l = H_l(x_{l-1}) \tag{9}$$

In equation (9), x_{l-1} is the input of layer $l-1$. x_l is the input of layer l. However, if the number of layers is too many, ResNet is often prone to the problem of vanishing gradient. The traditional ResNet is often improved by utilizing jump connections, which are shown in equation (10).

$$x_l = H_l(x_{l-1}) + x_{l-1} \tag{10}$$

Multiple residual blocks and jump connections are stacked by ResNet to help the model perform better by gradually learning the deeper properties of the input. However, as ResNet gets deeper and deeper at the same time, the gradient of the neural network may disappear, so the research proposes to improve it by utilizing LSTM. LSTM is a special RNN architecture, which is generally suitable for tasks that need to deal with long sequential data and long-term dependencies, and the gating mechanism and memory unit of LSTM enable the network to learn and memorize the information better [28], [29], [30]. Figure 4 depicts the architecture of the Res-LSTM network built for the study.

As shown in Figure 4, the study first introduces LSTM units in the residual block so that the model can better capture

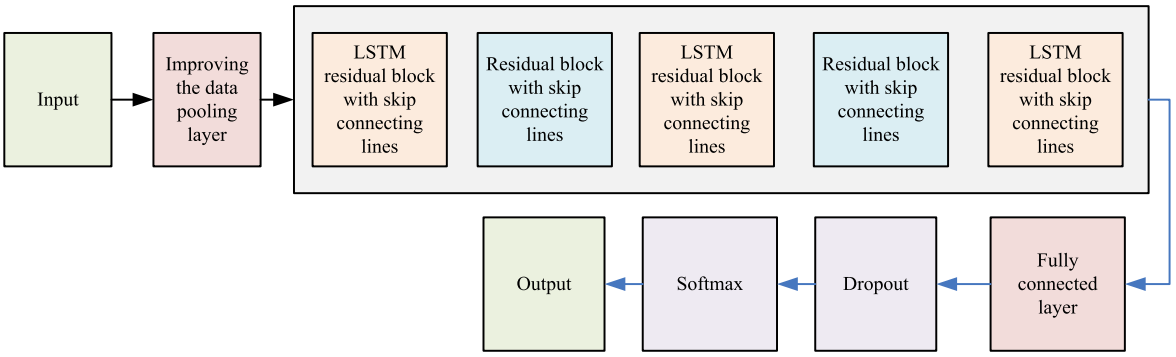

FIGURE 4. The Res-LSTM network structure.

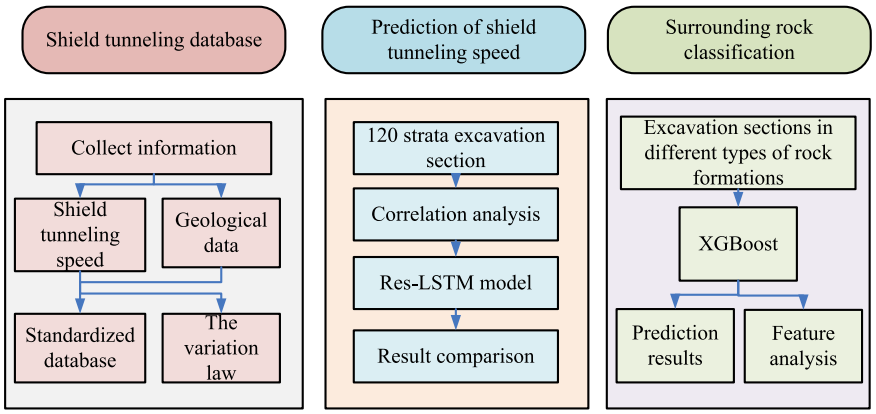

FIGURE 5. Basic framework of the prediction model of underground shield tunneling speed based on improved ResNet.

long-term dependencies. By controlling the information flow via the LSTM's gating mechanism, this hybrid structure can be made to process sequential data more efficiently on the network. The study then integrates LSTM units with ResNet's jump connections to enable information to move through the network more quickly, thereby mitigating the gradient vanishing problem and enhancing the network's training accuracy and efficiency. Finally, before the activation function, the study utilizes batch normalization to improve it. When the input function is $B\{x_{1,\ldots,m}\}$, its training parameter γ is calculated as shown in equation (11).

$$\mu_B \leftarrow \frac{1}{m}\sum_{i=1}^{m} x_i' \tag{11}$$

In equation (11), μ denotes the mean value. Equation (12) displays the training parameter formula.

$$\begin{cases} \sigma_B^2 \leftarrow \dfrac{1}{m}\displaystyle\sum_{i=1}^{m}(x_i' - \mu_B)^2 \\ \hat{x}_i' \leftarrow \dfrac{x_i' - \mu_B}{\sqrt{\sigma_B^2 + \varepsilon}} \end{cases} \tag{12}$$

In equation (12), σ denotes the standard deviation, ε denotes the constant, and m denotes the number. Subsequently, the back-standardization calculation is performed, which is shown in equation (13).

$$y_i' \leftarrow \gamma' \hat{x}_i' + \beta \equiv BN_{\gamma,\beta(x_i)} \tag{13}$$

To accomplish the parameter correction, this phase aims to reconvert the normalized data to the original data's range and scale. The output results are calculated as shown in equation (14).

$$\{y_i' \equiv BN_{\gamma,\beta(x_i)}\} \tag{14}$$

C. CONSTRUCTION OF DIGGING SPEED PREDICTION MODEL FOR DOWN-HOLE SHIELD MACHINE BASED ON IMPROVED RESNET

After completing the construction of coal mine down-hole GGPM model and Res-LSTM, the study combines the two to construct the DS prediction model of down-hole SM based on improved ResNet. The basic framework of the DS prediction model for down-hole SM based on improved ResNet constructed by the study is shown in Figure 5.

As shown in Figure 5, the DS prediction model of underground SM constructed by the study consists of SM digging database, DS prediction of SM and GGPM model of coal mine underground. In this model, the initial step involves the collection of detailed geological data and tunneling data

from the shield tunneling database. Subsequently, the study conducted a meticulous data cleansing process on the original data to guarantee the precision and dependability of the data. Subsequently, in order to ensure uniformity and facilitate processing, the research employs the MinMax standardization method to process the cleaned data. To assess the performance and generalization capacity of the model, the data set is divided into three distinct subsets: a training set, a validation set and a test set. Secondly, in constructing the prediction model of tunneling velocity for SMs, the stratum of the tunneling section that is most closely related to tunneling velocity is selected as the input parameter. Subsequently, two deep learning models, ResNet and LSTM, are integrated to construct the prediction model. The residual structure of ResNet enables the model to learn deeper feature representations, while LSTM is well-suited to processing time series data and capturing the temporal dynamics of the tunneling speed of the SM. Subsequently, the Res-LSTM model is trained on the training set, and the hyper-parameters of the model are adjusted on the verification set to achieve the optimal prediction performance. Subsequently, the XGBoost algorithm is employed to examine the distinctive characteristics of various grades of rocks. XGBoost is an efficient gradient lifting DT algorithm that is capable of automatically identifying correlations between features and eliminating redundant features, thereby enhancing the predictive power of the model. By comparing the prediction results of different input parameters, an optimal surrounding rock classification model can be constructed. Finally, the prediction model for SM driving speed and the prediction model for underground rock and soil grade are integrated. The combination method enables the model to consider the influence of geological information and engineering parameters on the driving speed of the SM simultaneously, thereby enhancing the accuracy and reliability of the prediction. The basic structure of the DS prediction model for down-hole SM based on improved ResNet constructed by the study is shown in Figure 6.

As shown in Figure 6, the basic architecture of the study to construct a ResNet -LSTM DS prediction model for down-hole SM combines the characteristics of ResNet and LSTM. In the data input layer, the study inputs the geological information, engineering parameters, and other features of down-hole SM to form a temporal data sequence. In the ResNet module, the study uses the ResNet module to process the spatio-temporal features. The residual structure of ResNet helps to train the deep network and facilitates the capture of complex nonlinear relationships. Subsequently, the study introduces an LSTM layer on top of the ResNet output to better capture temporal dependencies. The LSTM module can effectively learn and memorize long-term dependencies in temporal data, which is suitable for dealing with DS with temporal features in down-hole SM. Finally, the output layer is used to predict the DS of down-hole SM. In addition, to verify the validity of the DS prediction model of down-hole SM constructed by the study, the study also uses the confusion matrix as an evaluation tool. A two-dimensional table called

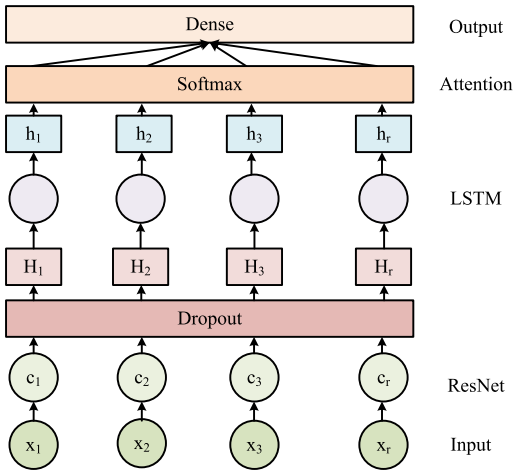

FIGURE 6. Basic structure of the prediction model of underground shield tunneling speed based on improved ResNet.

Confusion matrix		Real value	
		Positive	Negative
Predicted value	Positive	TP	FP
	Negative	FN	TN

FIGURE 7. The confusion matrix.

a confusion matrix is used to compare the discrepancies between real data and model projections. False positive (FP), false negative (FN), true positive (TP), and true negative (TN) are these. In Figure 7, the confusion matrix is displayed.

The confusion matrix makes it possible for the study to evaluate the model's performance in all respects, including prediction accuracy, performance in the event of positive and negative category imbalance, and information on categorization mistake.

IV. EMPIRICAL ANALYSIS OF DIGGING SPEED PREDICTION MODEL FOR DOWN-HOLE SHIELD MACHINE BASED ON IMPROVED RESNET

The work conducts performance comparison experiments and empirical assessments of the proposed SRT prediction model, the enhanced ResNet algorithm, and the DS prediction model for down-hole SM based on the improved ResNet, respectively, to confirm their efficacy.

A. VALIDATION OF THE EFFECTIVENESS OF THE XGBOOST SURROUNDING ROCK TYPE PREDICTION MODEL

The study verifies the effectiveness of the proposed XGBoost SRT prediction model through performance comparison experiments with a validation set taken from the Kaggle fenestration dataset. The convolutional neural network (CNN)

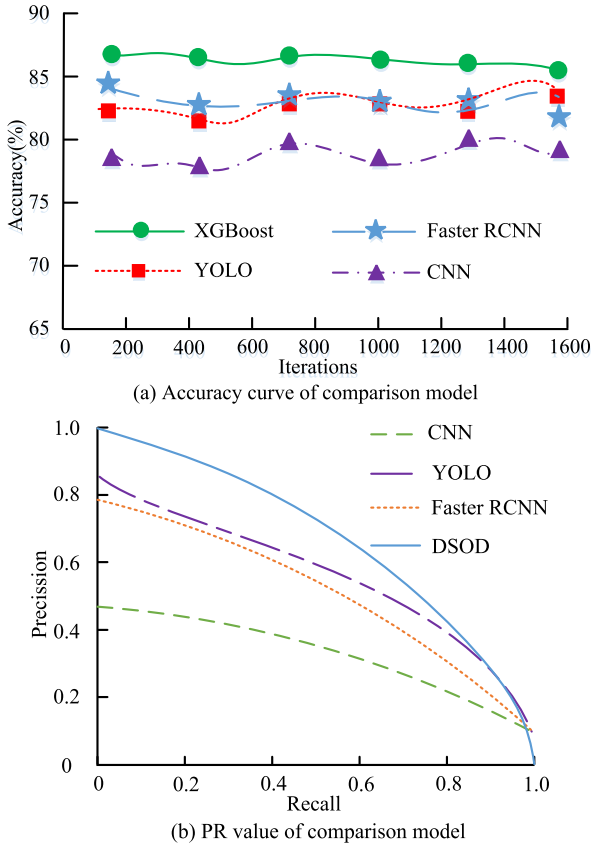

FIGURE 8. Accuracy and precision of the comparison results of each comparison model.

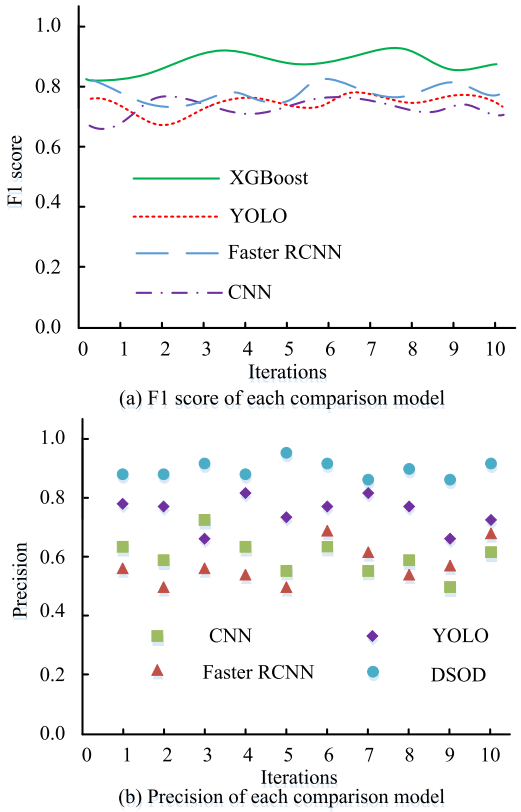

FIGURE 9. The F1 value and accuracy comparison results of each comparison model.

based SRT prediction models, the faster region-based convolutional neural network (Faster RCNN), and the you only look once (YOLO) model are the comparative models. The performance comparison metrics are accuracy, precision recall (PR) curve, F1 value, precision, error value and loss function value. The experimental environment is Matlab. Figure 8 displays the accuracy and precision comparison outcomes for each comparison model.

Figure 8 shows the accuracy and PR curves for each comparative model. Figure 8(a) shows the accuracy curves for each comparison model. Figure 8(a) shows how each comparison model's accuracy rises with the number of iterations. The study's suggested XGBoost SRT prediction model has an accuracy curve that is generally greater than the other models', with an average accuracy of 87.4%. The PR curve of the research-proposed XGBoost SRT prediction model, shown in Figure 8(b), has the biggest area under the line (0.78) compared to the other models. When the findings are summed up, it is evident that the research's suggested XGBoost SRT prediction model performs better in terms of accuracy. Figure 9 shows the results of F1 value and accuracy comparison for each comparison model.

The comparative findings of the F1 values for each SRT prediction model are displayed in Figure 9(a). With an F1 value of 0.86—which is 0.08 higher than the YOLO SRT prediction model—the study-proposed XGBoost SRT prediction model is overall superior to the other examined algorithms in Figure 9(a). The accuracy of the suggested XGBoost SRT prediction model is 0.04 higher than the YOLO SRT prediction model and 0.84 higher than that of other comparison algorithms, as shown in Figure 9(b). In conclusion, it is evident that the suggested XGBoost SRT prediction model outperforms the other SRT prediction models in terms of prediction performance and has use in real-world scenarios. Figure 10 displays the comparison outcomes of the error values and loss function values for every comparison model.

Figure 10(a) shows the comparative results of the error values of the comparison models. In Figure 10(a), the suggested XGBoost SRT prediction model has an error value curve that is lower overall than the other comparison models, and its average error is lower than the other SRT prediction models at 12.6%. Additionally, this model has greater stability and a lesser fluctuation amplitude of its error curve than the other comparative models. The results of comparing the loss function values of the comparison models are displayed in Figure 10(b). Each model's loss function value reduces as the number of iterations increases until it stabilizes. Nonetheless, the suggested XGBoost SRT prediction model's loss function value, which is 0.2, is generally less than that of the other comparison models. The suggested XGBoost SRT prediction model outperforms the other models in terms of stability and

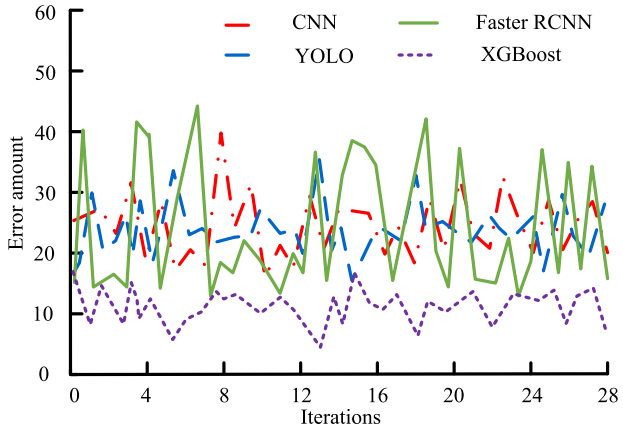

(a) Comparison results of the target extraction error value of each comparison model

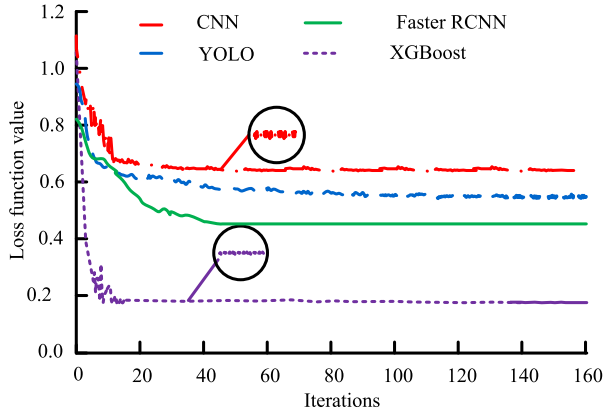

(b) Comparison results of the loss function value of each comparison model

FIGURE 10. Comparison results of the target extraction error value and the loss function value of each comparison model.

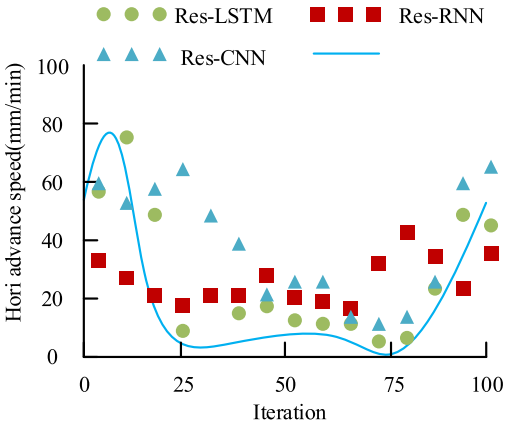

(a) The error values of each algorithm in the training set

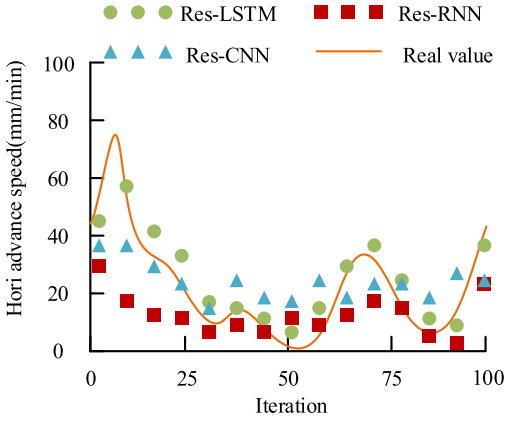

(b) The error values of each algorithm in the test set

FIGURE 11. Comparison results of the predicted value and the actual value of each comparison algorithm.

dependability, as can be observed from the summary of the preceding data.

B. VALIDATION OF THE EFFECTIVENESS OF THE MODIFIED RESNET ALGORITHM INCORPORATING LSTM

The study performs performance comparison experiments on the UCI dataset as a validation set to verify the efficacy of the Res-LSTM algorithm presented in the study. The comparison algorithms are residual networks-convolutional neural network (Res-CNN) and residual networks-recurrent neural network (Res-RNN). The performance comparison metrics are error value, root-mean-square error (RMSE) and mean absolute error (MAE) and coefficient of determination (R^2). Matlab serves as the experimental environment. Figure 11 displays the outcomes of comparing each comparison algorithm's anticipated and actual values.

Each comparison algorithm in the training set is shown with its error comparison results in Figure 11(a). The Res-LSTM algorithm developed by the study has a higher prediction value and a maximum deviation error value of 4.6 mm/min, which is better than the other comparison algorithms. The error comparison outcomes for every comparison algorithm in the test set are displayed in Figure 11(b). This figure illustrates how the highest deviation error value of the Res-LSTM algorithm, which is built for the study, is 2.2 mm/min, indicating higher prediction performance, and how its forecast value matches the real value more closely than the predicted values of the other comparison algorithms. Figure 12 displays the comparison results of the R^2, MAE, and RMSE values for each comparison algorithm.

Figure 12 (a) shows the prediction error results of Res-CNN, where RMSE value of Res-CNN algorithm is 2.052, MAE is 0.857, and R^2 is 0.959. RMSE is a standard measure of the discrepancy between the predicted value and the actual observed value. It is calculated by taking the mean square root of the square of the predicted value and the actual value, thereby giving greater weight to large errors. MAE is the mean of the absolute values of the deviations between all individual observations and the true value. In contrast to RMSE, MAE assigns equal weight to all errors, irrespective of their magnitude. R^2 is the coefficient of determination for regression analysis and is employed to quantify the degree to which the model fits the data. The closer the value is to 1, the closer the predicted value of the model is to the observed value. Figure 12 (b) presents the results of the prediction

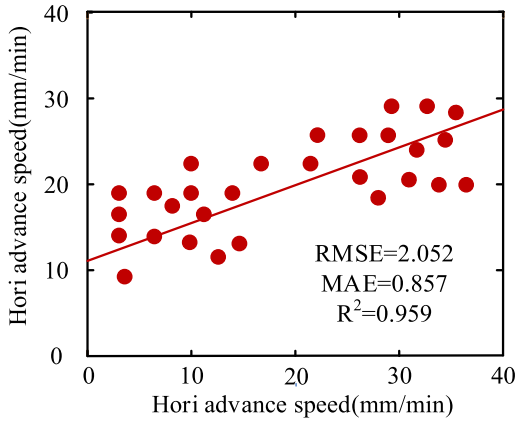

(a) Comparison of prediction results of Res-CNN

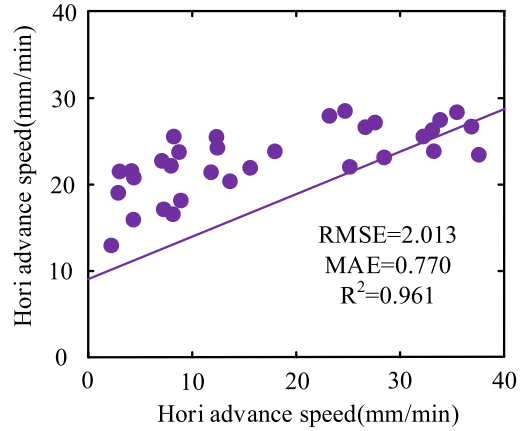

(b) Comparison of prediction results of Res-RNN

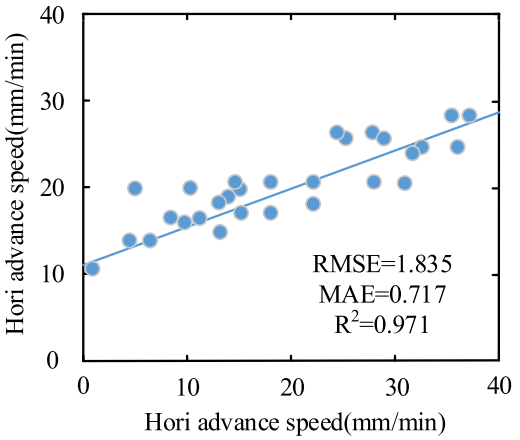

(c) Comparison of prediction results of Res-LSTM

FIGURE 12. Comparison results of the prediction error of each comparison algorithm.

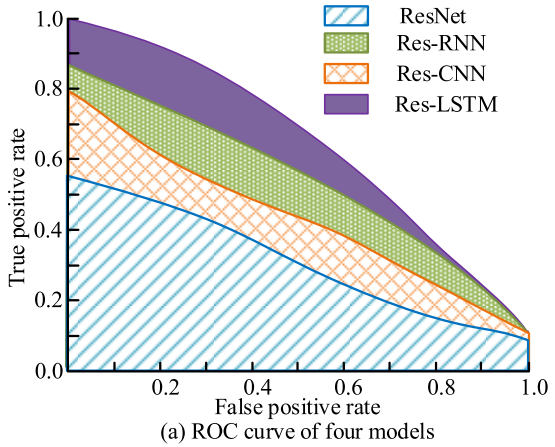

(a) ROC curve of four models

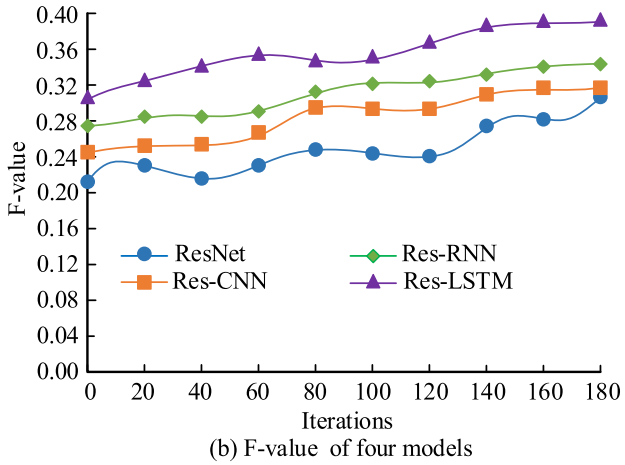

(b) F-value of four models

FIGURE 13. Comparison of the ROC curves and F1 values of each model.

error for Res-RNN, with an RMSE value of 2.013, which is slightly lower than that of Res-CNN. This indicates that the deviation of the predicted value of Res-RNN is slightly smaller than the actual observed value overall. Concurrently, the MAE of Res-RNN is 0.770, which is also lower than that of Res-CNN, indicating a smaller average absolute error. The R^2 value increased to 0.961, indicating that Res-RNN exhibited a slight improvement in the degree of fit between the data and the model. Figure 12 (c) shows the prediction error results of Res-LSTM. Among the three algorithms, Res-LSTM has the lowest RMSE value (1.835), indicating that its prediction results exhibit the least deviation from the actual value. In a similar manner, its MAE value is also the lowest (0.717), indicating the most accurate average accuracy. The R^2 value is the highest (0.971), indicating that the model has a high degree of fit to the data. In conclusion, the comparative analysis of RMSE, MAE, and R^2 indicates that Res-LSTM exhibits the most optimal predictive performance.

C. EMPIRICAL ANALYSIS OF DIGGING SPEED PREDICTION MODEL FOR DOWN-HOLE SHIELD MACHINE BASED ON RES-LSTM

To validate the performance of the DS prediction model for down-hole SM based on Res-LSTM, the study conducted a performance comparison test with the DS prediction model for down-hole SM based on Res-RNN, Res-CNN and traditional ResNet. The performance evaluation indexes are receiver operating characteristic curve (curve), F1 value, error, reaction time, RMSE and MAE. The dataset used is the constructed shield tunneling dataset. The experimental environment is Windows 10 and MATLAB platform.

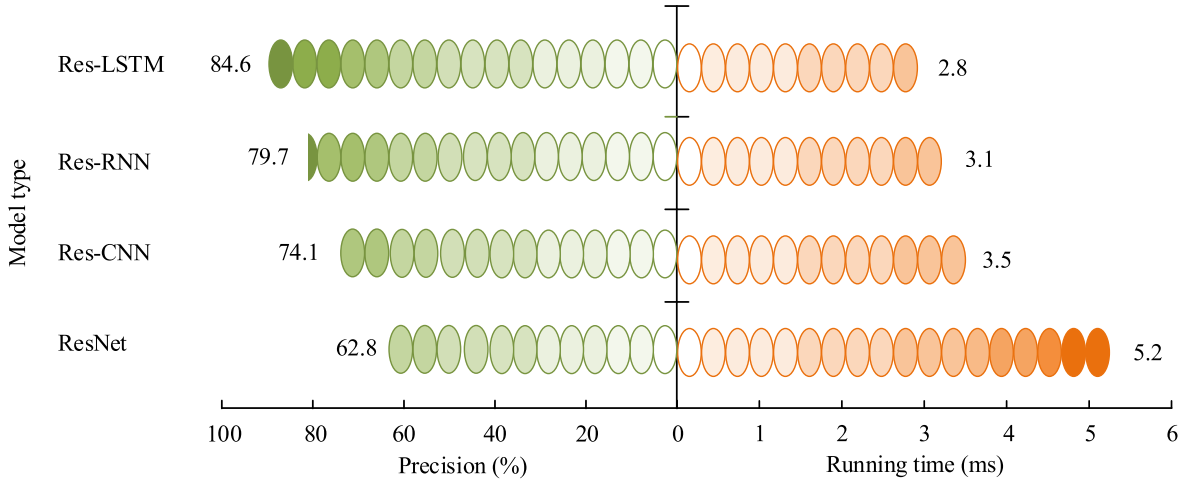

FIGURE 14. Accuracy and operation time of each model.

TABLE 1. RMSE, MAE and R^2 values of each comparison model.

Model	Data set	RMSE	MAE	R^2
ResNet	Training set	1.917	0.723	0.925
	Test set	2.052	0.857	0.902
Res-CNN	Training set	2.021	0.899	0.933
	Test set	1.980	0.715	0.913
Res-RNN	Training set	2.125	0.896	0.935
	Test set	2.013	0.771	0.915
Res-LSTM	Training set	1.972	0.736	0.967
	Test set	1.847	0.702	0.942

Figure 13 displays the ROC curves and F1 values for each model.

The ROC curves for the DS prediction models for each down-hole SM are displayed in Figure 13(a). The larger area under the ROC curve line of 0.74 for the recommended Res-LSTM DS prediction model for down-hole SM indicates that it has a stronger prediction effect than the other models. Figure 13(b) shows the F1 values of the DS prediction model for each down-hole SM. The F1 value of the proposed Res-LSTM DS prediction model for down-hole SM is 0.35, which is higher than that of the other m-models, indicating a better prediction performance for DS of down-hole SM. In conclusion, the findings demonstrate that the suggested Res-LSTM DS prediction model performs better for down-hole SM than alternative models. The accuracy and fault response time of each DS prediction model for down-hole SM are shown in Figure 14.

With a prediction accuracy of 84.6%, the DS prediction model suggested in the study for Res-LSTM down-hole SM outperforms the other comparison models by a wide margin, as seen in Figure 14. Furthermore, the model's response time of 2.8 s is noticeably faster than that of the other comparative models. In Summary, the DS prediction model of Res-LSTM for down-hole SM has higher accuracy and lower reaction time than the other models, and the model has high reliability and efficiency in DS prediction for down-hole SM. Table 1 displays the comparative findings of the R^2, MAE, and RMSE values for each comparison model.

Table 1 illustrates that the DS prediction model of Res-LSTM down-hole SM built by the study has a lower MAE of 0.736 and a lower RMSE value of 1.972 in the training set than the other comparison models and its R^2 is 0.967, which is significantly higher than the comparison model. In the test set, the RMSE value of the DS prediction model of Res-LSTM down-hole SM constructed by the study is 1.847, and the MAE is 0.702, which is smaller than the other comparison models and the R^2 is 0.942, which is significantly better than the comparison model. In conclusion, the findings demonstrate the superior performance and usefulness of the Res-LSTM down-hole SM DS prediction model developed by the research over previous comparative models.

V. CONCLUSION

The integration of the enhanced residual network of LSTM and ResNet, in conjunction with the XGBoost SRT prediction model, has led to a notable enhancement in the accuracy and efficacy of DS prediction for underground ore bodies. Furthermore, this integration has facilitated the advancement of the digitization process of coal mine production. In this study, LSTM and ResNet are integrated in order to enhance the residual network. The advantage of this method is that LSTM is well-suited to processing sequence data and capturing long-term dependencies in time series. The ResNet architecture effectively addresses the issue of gradient disappearance and model degradation in deep neural networks by incorporating residual learning. The combination of LSTM and ResNet has the potential to not only capture long-term dependencies in time series data, but also to enhance the depth of the network through residual learning, thereby improving the accuracy of prediction. This integrated method demonstrates

robust feature extraction and prediction capabilities when confronted with intricate and nonlinear underground ore body data. The adaptive learning of the deep learning model enables the extraction of useful information from a large amount of data in a more effective manner, thereby providing substantial support for the safety and efficiency of coal mine production. Through comparison experiments, it is found that the ROC curve area under the hybrid algorithm is 0.74, F1 value is 0.35, and the accuracy is as high as 84.6%, which is significantly better than other comparison models, and its maximum deviation error, RMSE and MAE are 4.6mm/min, 1.835 and 0.717, respectively. Furthermore, the enhanced algorithm was integrated with the XGBoost SRT prediction model, which is a highly efficient gradient lifting DT algorithm with exceptional predictive performance and computational efficiency. The study integrated deep learning models to leverage XGBoost's proficiency in handling structured data and deep learning's aptitude for navigating intricate nonlinear relationships. This combination enabled the model to accommodate both traditional statistical characteristics and to discern intricate patterns within the data. Through empirical analysis, it is found that the RMSE value of this model is 1.847, MAE is 0.702, which is smaller than other comparison models, and the R^2 value of 0.942 is also superior to that of the comparison model, thereby substantiating the efficacy and applicability of the model in question. However, this study also has some limitations. It only discusses the prediction of excavation speed with the input characteristics of the model as excavation parameters, but does not carry out sensitivity analysis of engineering geological parameters. The future research direction is to combine geological parameters and shield driving parameters to predict the driving speed of the SM and predict the driving speed of the shield.

REFERENCES

[1] B. Wang, R. Santoreneos, L. Giles, H. Haji Ali Afzali, and H. Marshall, "Case fatality rates of invasive meningococcal disease by serogroup and age: A systematic review and meta-analysis," *Vaccine*, vol. 37, no. 21, pp. 2768–2782, May 2019, doi: 10.1016/j.vaccine.2019.04.020.

[2] Z. Chen and P. D. Boves Harrington, "Self-optimizing support vector elastic net," *Anal. Chem.*, vol. 92, no. 23, pp. 15306–15316, Nov. 2020, doi: 10.1021/acs.analchem.0c01506.

[3] K. B. Deatrick, M. A. Mazzeffi, S. M. Galvagno, R. B. Tesoriero, D. J. Kaczoroswki, D. L. Herr, K. Dolly, R. P. Rabinowitz, T. M. Scalea, and J. Menaker, "Outcomes of venovenous extracorporeal membrane oxygenation when stratified by age: How old is too old?" *ASAIO J.*, vol. 66, no. 8, pp. 946–951, Aug. 2020, doi: 10.1097/mat.0000000000001076.

[4] H. Saxena, A. Singh, and J. N. Rai, "Adaptive spline-based PLL for synchronisation and power quality improvement in distribution system," *IET Gener., Transmiss. Distrib.*, vol. 14, no. 7, pp. 1311–1319, Apr. 2020, doi: 10.1049/iet-gtd.2019.0662.

[5] S. Yniesta and M. Janati-Idrissi, "Integration of viscoplastic effects in a one-dimensional constitutive model for ground response analysis," *Can. Geotech. J.*, vol. 58, no. 4, pp. 468–478, Apr. 2021, doi: 10.1139/cgj-2019-0717.

[6] B. K. Gao, L. Dong, H. B. Bi, and Y. Z. Bi, "Focus on temporal graph convolutional networks with unified attention for skeleton-based action recognition," *Appl. Intell.*, vol. 52, no. 5, pp. 5608–5616, Aug. 2022, doi: 10.1007/s10489-021-02723-6.

[7] M. Ota, H. Tateuchi, and T. Hashiguchi, "Verification of validity of gait analysis systems during treadmill walking and running using human pose tracking algorithm," *Gait Posture*, vol. 85, no. 1, pp. 290–297, Mar. 2021, doi: 10.1016/j.gaitpost.2021.02.006.

[8] F. Xue, H. Ji, and W. Zhang, "Mutual information guided 3D ResNet for self-supervised video representation learning," *IET Image Process.*, vol. 14, no. 13, pp. 3066–3075, 2020, October, doi: 10.1049/iet-ipr.2020.0019.

[9] W. M. Salama, A. M. Elbagoury, and M. H. Aly, "Novel breast cancer classification framework based on deep learning," *IET Image Process.*, vol. 14, no. 13, pp. 3254–3259, Oct. 2020, doi: 10.1049/iet-ipr.2020.0122.

[10] O. M. Lawal and H. Zhao, "YOLOFig detection model development using deep learning," *IET Image Process.*, vol. 15, no. 13, pp. 3071–3079, Jun. 2021, doi: 10.1049/ipr2.12293.

[11] J. Chen, J. Q. Li, T. Li, H. G. Liu, and Y. Z. Wang, "Rapid identification of the storage duration and species of sliced boletes using near-infrared spectroscopy," *J. Food Sci.*, vol. 87, no. 7, pp. 2908–2919, Jun. 2022, doi: 10.1111/1750-3841.16220.

[12] Z. Yang, X. Zheng, X. Gao, Q. Zeng, C. Yang, J. Luo, C. Zhan, and Y. Lin, "Deep learning methodology for obtaining ultraclean pure shift proton nuclear magnetic resonance spectra," *J. Phys. Chem. Lett.*, vol. 14, no. 14, pp. 3397–3402, Mar. 2023, doi: 10.1021/acs.jpclett.3c00455.

[13] Y. Fang, J. Cui, D. Wanatowski, N. Nikitas, R. Yuan, and Y. He, "Subsurface settlements of shield tunneling predicted by 2D and 3D constitutive models considering non-coaxiality and soil anisotropy: A case study," *Can. Geotech. J.*, vol. 59, no. 3, pp. 424–440, Mar. 2022, doi: 10.1139/cgj-2020-0620.

[14] H. Gao, Q. Wang, B. Jiang, P. Zhang, Z. Jiang, and Y. Wang, "Relationship between rock uniaxial compressive strength and digital core drilling parameters and its forecast method," *Int. J. Coal Sci. Technol.*, vol. 8, no. 4, pp. 605–613, Jan. 2021, doi: 10.1007/s40789-020-00383-4.

[15] Z. Zhang, M. Huang, C. Zhang, K. Jiang, and Q. Bai, "Analytical prediction of tunneling-induced ground movements and liner deformation in saturated soils considering influences of shield air pressure," *Appl. Math. Model.*, vol. 78, pp. 749–772, Feb. 2020, doi: 10.1016/j.apm.2019.10.025.

[16] M. Jasemi, S. Hessabi, and N. Bagherzadeh, "Enhancing reliability of emerging memory technology for machine learning accelerators," *IEEE Trans. Emerg. Topics Comput.*, vol. 9, no. 4, pp. 2234–2240, Apr. 2021, doi: 10.1109/TETC.2020.2984992.

[17] Q. Wang, X. Xie, and I. Shahrour, "Deep learning model for shield tunneling advance rate prediction in mixed ground condition considering past operations," *IEEE Access*, vol. 8, pp. 215310–215326, 2020, doi: 10.1109/ACCESS.2020.3041032.

[18] Y. Wang, R. Xiong, P. Tang, and Y. Liu, "Fast and reliable map matching from large-scale noisy positioning records," *J. Comput. Civil Eng.*, vol. 37, no. 1, pp. 1–14, Sep. 2023, doi: 10.1061/(ASCE)CP.1943-5487.0001054.

[19] L. Junyu, H. Zeyao, L. Jiaxin, Z. Yousheng, and X. Xiaobao, "Compositional gradient engineering and applications in halide perovskites," *Chem. Commun.*, vol. 59, no. 35, pp. 5159–5173, Mar. 2023, doi: 10.1039/D3CC00967J.

[20] E. Nsugbe, "Toward a self-supervised architecture for semen quality prediction using environmental and lifestyle factors," *Artif. Intell. Appl.*, vol. 1, no. 1, pp. 35–42, Sep. 2022, doi: 10.47852/bonviewaia2202303.

[21] W. He, S. A. Bagherzadeh, and M. Tahmasebi, "A new method of black-box fuzzy system identification optimized by genetic algorithm and its application to predict mixture thermal properties," *Int. J. Numer. Methods Heat Fluid Flow*, vol. 30, no. 5, pp. 2485–2499, October, Oct. 2019, doi: 10.1108/HFF-12-2018-0758.

[22] S. Khademolqorani, "Quality mining in a continuous production line based on an improved genetic algorithm fuzzy support vector machine (GAFSVM)," *Comput. Ind. Eng.*, vol. 169, Jul. 2022, Art. no. 108218, doi: 10.1016/j.cie.2022.108218.

[23] R. Pongen, A. K. Birru, and P. Parthiban, "Optimal design of die casting process parameters of A713 cast alloy with grain refinement by using genetic algorithm approach for automobile industries," *Int. J. Heavy Vehicle Syst.*, vol. 29, no. 2, pp. 197–211, Aug. 2022, doi: 10.1504/IJHVS.2022.125309.

[24] J. Shen, C. Du, F. Yan, B. Chen, and Z. Tu, "Two parameters identification for polarization curve fitting of PEMFC based on genetic algorithm," *Int. J. Energy Res.*, vol. 46, no. 7, pp. 9621–9633, Mar. 2022, doi: 10.1002/er.7831.

[25] F. Cappelletti, M. Rossi, and M. Germani, "How de-manufacturing supports circular economy linking design and EoL—A literature review," *J. Manuf. Syst.*, vol. 63, pp. 118–133, Apr. 2022, doi: 10.1016/j.jmsy.2022.03.007.
[26] H. Liu, R. Guensler, H. Lu, Y. Xu, X. Xu, and M. O. Rodgers, "MOVES-matrix for high-performance on-road energy and running emission rate modeling applications," *J. Air Waste Manage. Assoc.*, vol. 69, no. 12, pp. 1415–1428, Dec. 2019, doi: 10.1080/10962247.2019.1640806.
[27] A. M. Nasrabadi and M. Moghimi, "Energy analysis and optimization of a biosensor-based microfluidic microbial fuel cell using both genetic algorithm and neural network PSO," *Int. J. Hydrogen Energy*, vol. 47, no. 7, pp. 4854–4867, Jan. 2022, doi: 10.1016/j.ijhydene.2021.11.125.
[28] M. Mohammadian, "Application of the modified Fourier series method and the genetic algorithm for calibration of small-scale parameters in the nonlocal strain gradient nanobeams," *Math. Methods Appl. Sci.*, vol. 45, no. 10, pp. 6325–6345, Feb. 2022, doi: 10.1002/mma.8173.
[29] R. M. Kakhki, M. Mohammadpoor, and R. Faridi, "The development of an artificial neural network–genetic algorithm model (ANN-GA) for the adsorption and photocatalysis of methylene blue on a novel sulfur–nitrogen co-doped Fe_2O_3 nanostructure surface," *RSC Adv.*, vol. 10, no. 10, pp. 5951–5960, Feb. 2020, doi: 10.1039/C9RA10349J.
[30] Y. Y. Hong, Y. H. Chan, and Y. H. Cheng, "Week-ahead daily peak load forecasting using genetic algorithm-based hybrid convolutional neural network," *IET Gener., Transmiss. Distrib.*, vol. 16, no. 12, pp. 2416–2424, Mar. 2022, doi: 10.1049/gtd2.12460.

HUIGANG XU was born in Jinzhong, Shanxi, China, in June 1985. He received the bachelor's degree in mining engineering from China University of Mining and Technology, in 2007, and the master's degree in mining engineering from the School of Safety Engineering, Key Laboratory of Gas and Fire Control for Coal Mines, China University of Mining and Technology, in 2013, where he is currently pursuing the Ph.D. degree in safety engineering.

From 2007 to 2013, he was a Technician with Shanxi Xinyuan Coal Company Ltd. He was an Assistant level employee, a first level employee, the Chief Engineer, and the Director of the Chief Engineer's Office, Shanxi Xinyuan Coal Company Ltd., from 2013 to 2014, from 2014 to 2017, from 2017 to 2018, and from 2018 to 2019, respectively. Since 2019, he has been the Chief Engineer of Shanxi Xinyuan Coal Company Ltd. As the main person in charge of technical management, he vigorously implements the technology innovation driven strategy, mainly promoting the Y-shaped ventilation along the goaf, the "three highs and one low" support technology, surface water and sand fracturing, full face shield tunneling machine rock roadway fast excavation, bottom plate rock roadway through layer drilling to protect coal and rock, and other new technologies and equipment applications. He comprehensively promotes the deep development of technological innovation with Xinyuan Company and promotes the high-quality development of the enterprise. He has published ten scientific and technological articles, led and participated in 12 scientific research projects, and applied for eight patents.

Mr. Xu won one second prize of Shanxi Province Science and Technology Progress Award, five second prizes of China Coal Industry Association Science and Technology Progress Award, and two third prizes. He won titles, such as the 2023 Coal Youth Science and Technology Award and the Outstanding Young Chief Engineer in the Coal Industry.

XUYAO QI was born in Suining, Jiangsu, in November 1984. He received the bachelor's degree in fire protection engineering from China University of Mining and Technology (CUMT), in 2006, and the joint Ph.D. degree in safety technology and engineering from CUMT and the University of Maryland, USA, in 2011.

After graduation in 2011, he was with the School of Safety Engineering, Key Laboratory of Gas and Fire Control for Coal Mines, China University of Mining and Technology, and was promoted to an Associate Professor, in December 2013. Then, he was promoted to a Professor, in December 2018. He has been the Deputy Director of the International Research Center for Underground Gasification of Coal, since 2016, and the Key Laboratory of Coal Mine Gas and Fire Prevention and Control of the Ministry of Education, since 2020. He has published two academic monographs, authorized 22 national invention patents, and has published more than 80 academic articles. In recent years, he presided over four National Natural Science Foundation of China projects, China Postdoctoral Science Foundation, Jiangsu Provincial Natural Science Foundation Surface projects, and two subtopics of the National Key Research and Development Program projects. His research interests include ventilation and fire prevention and suppression, occupational safety and health, fire protection and emergency rescue, and fluidized coal mining. His current research interests include mine ventilation and fire prevention and suppression, and underground space fire prevention and protection.

Prof. Qi was selected for the National Major Talent Project Youth Program and the National University Award for Outstanding Young Scientific and Technological Talents in the field of mining and petroleum safety engineering. His achievements were honored with the Second Prize of Sichuan Provincial Scientific and Technological Progress and the Second Prize of Jiangsu Provincial Science and Technology Award.

ZHONGQIU LIANG was born in Shenyang, Liaoning, China, in August 1987. He received the bachelor's degree in safety engineering from Southwest University of Science and Technology, in 2010, and the master's degree in safety engineering and technology from Shenyang Research Institute, Coal Science Research Institute, in 2014.

Since August 2011, he has been with the Gas Research Branch of Middling Coal Science and Engineering, CCTEG Shenyang Research Institute, where he was engaged in mining safety, as the Project Manager. He has been the Project Manager in Yangquan mining area. Since joining the job, he has been deeply involved in the technical guidance and service of gas prevention and utilization in high gas and prominent mining areas in China for a long time, making contributions to ensuring coal mine safety production and people's health and life. For many years, he has led a team to tackle technological bottlenecks in the prevention and utilization of gas in high outburst coal seams, committed to solving gas control problems that constrain coal mine safety production. He has published 20 articles in national professional journals, led and participated in two major national science and technology projects, led and participated in more than 20 horizontal technical consulting and gas control engineering projects, applied for nine patents, and participated in two standards under compilation. He has participated in multiple major gas control projects and technical service projects, solving practical gas control problems for corresponding coal mines and achieving good economic benefits for the unit.

Mr. Liang won four provincial and ministerial level science and technology awards and two group company technology application awards.